PARAMETER INFLUENCE ANALYSIS OF BALL MILL BASED ON DEM

Jinfeng ZHANG[1], Tie QU[2]*, Bijuan YAN[1], Chunjiang ZHAO[1], Qiang BIAN[1], Zhangda ZHAO[1], Biliang TANG[2]

Liner ripple height and rotational rate are two important parameters which will influence the grinding efficiency of ball mill. In order to choose them reasonably, the dynamics equation of grinding media is established. Then the discrete element model of ball mill with waveform liner is built. The correctness of the established model was verified by comparing it with the experimental data in the literature [16]. The influences of liner ripple height and rotational rate on the collisions number and useful power as well as impact force are analyzed. The results show that with the increase of rotation rate and corrugation height, the number of collisions between steel balls and ores, impact force and useful power all show a trend of first increasing and then decreasing, while the number of collisions between steel balls shows a trend of first decreasing and then increasing, the best rotational rate is between 70% and 90%, and the best corrugation height is between 100mm and 140mm. The results of this paper can provide some reference for the optimization of ball mill parameters.

Keywords: ball mill; ripple height; rotational rate; DEM.

1. Introduction

Ball mills are widely used in the production of minerals and powders and have the advantages of large crushing ratio, good crushing effect and high applicability. But the problems such as low efficiency, high steel ball consumption and liner grinding loss always exist [1-2]. The low efficiency is closely related to their liners' design and rotation rate which is equal to the ratio of the rotational speed and critical speed of ball mills [3-6]. However, the influence mechanism of such factors is not grasped clearly up to now.

To solve above-mentioned questions, the shape and structural parameters as well as numbers of the liners have been studied by many researchers. For example, Weerasekara et. al [7] studied the influence of the lifting bar height and face angle of trapezoidal liner on the motion state of the grinding media and proposed the design basis of the liner in combination with Davis theory. Liang et. al [8] analyzed the motions of grinding media inside a positive polygon angle

[1] Mr., School of Mechanical Engineering College, Taiyuan University of Science and Technology, China, e-mail: zjf15735044589@126.com.
[2] Eng., CITIC Heavy Industries Co., Ltd, Luoyang,471039, China.
* E-mail: qutie3563@126.com.

spiral liner and studied the effect of positive polygon angle spiral liner on the efficiency of the ball mill. Wang and Sun et. al [9-10] studied the concave arc of the waveform liner and then optimized the parameters of the liner. From the literature search, it could be known that the effect of different ripple heights of waveform liners on efficiency of ball mills are seldom studied.

In addition, rotational rate of ball mills has also a great influence on their efficiency. With the increase of the rotation rate, the motion of grinding media is divided into lagging, throwing and centrifugal motion. When the grinding media is in centrifugal motion, the mill does useless work, which would seriously affect the grinding efficiency of the mill. To solve this problem, many studies have been carried out by related scholars. For example, Li [11] studied the effect of rotation rate on the motion and internal collision of the steel-ball and pointed out that as the rotation rate increased, the numbers of steel-ball in falling motion increased significantly and so the efficiency of the whole machine increased. Cleary et. al [12-14] predicted particle flows in grinding processes using DEM. However, the mechanism of the effect of rotation rate on the efficiency of waveform liner ball mill under different ripple heights was still not clear.

In this paper, the kinetic equations of grinding media are derived, in which the structural parameters of the corrugated liner are contained. And then a discrete element model of the corrugated liner is built based on EDEM. More importantly, the effects of different corrugation heights and rotational rates on the number of particle collisions, useful power, and impact force are analyzed. Therefore, the effects of different corrugation heights and rotational rate on grinding efficiency are grasped. The results in the paper could lay a theoretical foundation for further research on ball mills. And an increase efficiency in the grinding process could enhance the competitiveness of the products.

2. Kinetic equations of grinding media

The ball mill mainly crushes the ore through the impact force generated by the throwing motion of the grinding media. Therefore, the impact force is an important parameter for the ball mill. It can be obtained by analyzing the detachment angle of the outermost grinding media. The grinding media is considered as a "mass system". At the same time, the following assumptions are made: there is no friction between the grinding media; there is no relative sliding between the grinding media and liner in the rising zone. So the effect of sliding friction is ignored. Fig. 1 shows the interaction forces of a representative point A of the outermost grinding media. In Fig. 1, the point O stands for the center of the ball mill, and the point O_1 is the center of the concave arc on the liner.

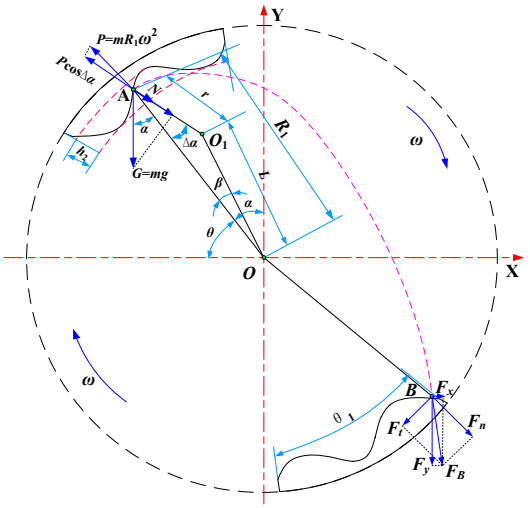

Fig. 1. Force analysis of grinding media (point *A*)

The equilibrium equation of the interaction forces on point *A* could be written as:

$$G + P + N = 0 \tag{1}$$

where *G*, *P*, *N* are the gravitational force of the point *A*, the centrifugal force generated by the rotation of the mill, and the normal force which is exerted by the inner wall of the liner, respectively. The projection of each vector in Eq. (1) in the line AO_1 is given as follows:

$$G\cos(\alpha + \Delta\alpha) + N - P\cos\Delta\alpha = 0 \tag{2}$$

where α is the detachment angle of grinding media, i.e. the angle between the line *OA* and *Y*-axis; $\Delta\alpha$ is the angle between the line *OA* and O_1A. Here, it should be noted that the normal force *N* changes continuously with the rotation of the mill. When *N*=0, the grinding media starts to break away from the inner wall of the liner. At this time, the following equation can be obtained:

$$mg\cos(\alpha + \Delta\alpha) - mR_1\omega^2\cos\Delta\alpha = 0 \tag{3}$$

where ω is the angular velocity of ball mill; *g* is the gravity acceleration. R_1 is the gyration-radius of point *A*.

Therefore, from the Eq. (3), the detachment angle α can be obtained as:

$$\alpha = \arccos\left(\frac{R_1\omega^2}{g}\cos\Delta\alpha\right) - \Delta\alpha \tag{4}$$

in addition, the relationship between β and $\Delta\alpha$ in Fig.1 can be obtained according to the sine theorem, it is shown as:

$$\frac{L}{\sin\Delta\alpha} = \frac{r}{\sin\beta} \tag{5}$$

$$\Delta\alpha = \arcsin\left(\frac{L}{r}\sin\beta\right) \tag{6}$$

where L is the distance from the liner's mass center O_1 to the mill center O; r is the ripple radius of the waveform liner. β is the angle between the line AO and OO_1.

At the same time, the gyration-radius of R_1 can be expressed as:

$$R_1 = L\cos\beta + \sqrt{r^2 - L^2\sin^2\beta} \tag{7}$$

and the horizontal and vertical components of the impact force could be obtained respectively as [15]:

$$F_x = \frac{\gamma h}{g}\omega^2 r_1^2 dr_1(\sin\theta + \sin 3\theta) \tag{8}$$

$$F_y = -\frac{\gamma h}{g}\omega^2 r_1^2 dr_1(3\cos\theta + \cos 3\theta) \tag{9}$$

where γ is the density of the micro-element; r_1 is the radius of the element; h is the length of the mill; θ is the central angle of the drop point; dr_1 is the amount by which r_1 varies infinitesimally.

From Figure. 1, it could be known that the range of β is [0, $\theta_1/3$], and the forces acting on the cylinder wall when the grinding media is in parabolic motion can be divided into tangential and normal forces.

According to the momentum theorem, the normal component force F_n can be described as:

$$F_n = dm(v_n - v_{dn}) \tag{10}$$

where θ_1 is the opening angle of the liner; dm is the mass thrown per unit time during the oblique throwing motion, and it can be expressed as: $dm=\gamma h\omega r_1 dr_1/g$; v_n is the initial normal velocity of the media at the landing point, which can be obtained as: $v_n=8v\sin 3\alpha\cos\alpha$; v is the impact velocity of the grinding media at the landing point; v_{dn} is the final normal velocity of the media at the footing point, with a value of 0.

Bringing dm, v_n, v_{dn} into Eq. (10), the values can be expressed as:

$$F_n = 8\frac{\gamma h}{g}v\sin^3\alpha\cos\alpha\omega r_1 dr_1 \tag{11}$$

since $\sqrt{F_x^2 + F_y^2} = \sqrt{F_n^2 + F_t^2}$, the tangential force F_t can be obtained as:

$$F_t = \sqrt{F_x^2 + F_y^2 - F_n^2} \tag{12}$$

3. EDEM Model of ball mill cylinder

The 3D model of the ball mill cylinder is created in SolidWorks, which is shown in Fig. 2 and its specific structural parameters are shown in Table 1. To simplify the calculation process, the threaded holes in the liner are omitted during the modeling of cylinder. The shape of the liner is shown in Fig. 3, in which the minimum thickness is expressed with h_1, h_1+h_2 is the maximum thickness.

Table 1

Ball mill parameters

Parameter	Code name	The numerical value
Cylinder diameter /mm	D_1	7320
Valid length / mm	h	1250
Effective inner diameter /mm	D_2	7166
Critical speed r/min	n_c	15.84
Media fill rate	φ	0.29
Liner thickness /mm	d	77
Steel ball quality /kg	m_1	38300
Media porosity	ξ	0.38

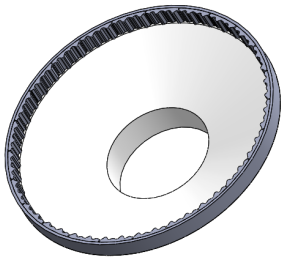

Fig. 2. Ball mill cylinder assembly drawing

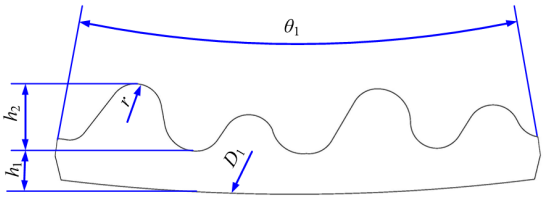

Fig. 3. Schematic diagram of the liner

The ball mill model which has been created in Solid works is imported into the EDEM. Next, the parameters of spherical particles and liner which are shown in Table 2 and Table 3 are added in the EDEM pre-processor. And the virtual particle plant and rotational speed are set. Finally, the contact type and gravity are also needed to be given. At this time, after the step and time of simulation as well as mesh size in the solver are given, the EDEM analysis may start. The discrete element model is shown in Fig. 4 (a).

Table 2

Size parameters of particles (media and ore)

	Grinding media			Ore		
Size /mm	ϕ60	ϕ80	ϕ50	ϕ70	ϕ90	ϕ100
Volume/cm3	904.78	2144.66	268.08	1436.76	3053.63	4188.79
ratio (%)	42.86	57.14	16.13	22.58	29.03	32.26
Total mass /kg	38300			14147		

Table 3

Material parameters of particles and liner

	Shear modulus E/Pa	Poisson's ratio v	Density/ (kg/m3)	Recovery factor	Static friction coefficient	Rolling friction coefficient
Steel balls	1e+10	0.3	7850	0.5	0.15	0.05
Liner	8.154e+10	0.3	7850	0.4	0.15	0.05
Ore	2.46e+07	0.27	3380	0.5	1.2	0.01

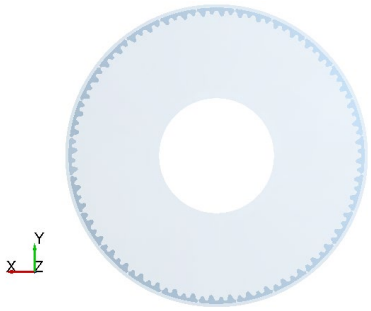

(a) Discrete element model of a ball mill cylinder with a waveform liner

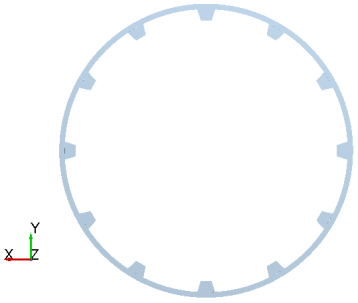

(b) Discrete element model of a ball mill cylinder with a trapezoidal liner

Fig. 4. Ball mill cylinder discrete element model

4. Model validation

To verify the correctness of the discrete element model of the ball mill constructed in this paper, the ball mill grinding media motion parameters and discrete element numerical simulation parameters mentioned in the literature [16] were selected for validation, and the basic parameters are shown in Table 4. The discrete element model is shown in Fig. 4 (b). In this case, the trapezoidal liner has an upper bottom of 20 mm, a lower bottom of 33 mm and a height of 20 mm in cross section. A comparison of the ball mill cylinder parameters for both is shown in Table 5.

Table 4

Basic parameters in literature [16]

Parameter	Numeric value	Parameter	Numeric value
Ball mill barrel diameter (mm)	520	Lift bar shape	trapezium
The barrel length of the ball mill (mm)	260	Iron ore density (kg/m3)	3883
Diameter of the grinding medium (mm)	30	Iron ore shear modulus (Pa)	2.6e+09
Iron ore granular grade (mm)	-9.5+6.7	Iron ore Poisson's ratio	0.25
Milling medium fill rate/φ1	30%	Diameter of the grinding medium (mm)	30
Iron ore filling rate/φ2	8%	Density of the grinding medium (kg/m3)	8842
Rotational rate/ψ	65%; 75%; 85%	Modulus of shear of the grinding medium (Pa)	7e+10

Table 5

Comparison of the ball mill parameters in this paper with those in the literature [16]

Parameters	This article Ball Mill	Literature [16] Ball mill
Cylinder size /mm	ϕ7166×1250	ϕ520×260
Type of liner	Corrugated liner	Trapezoidal liner
Number of liners	24	12
Critical speed /r/min	15.84	58.8

According to the basic parameters, a discrete element model of the trapezoidal liner ball mill is established, and the variation curves of the average power and average angular velocity of the ball mill with the rotation rate are obtained as shown in Fig. 5.

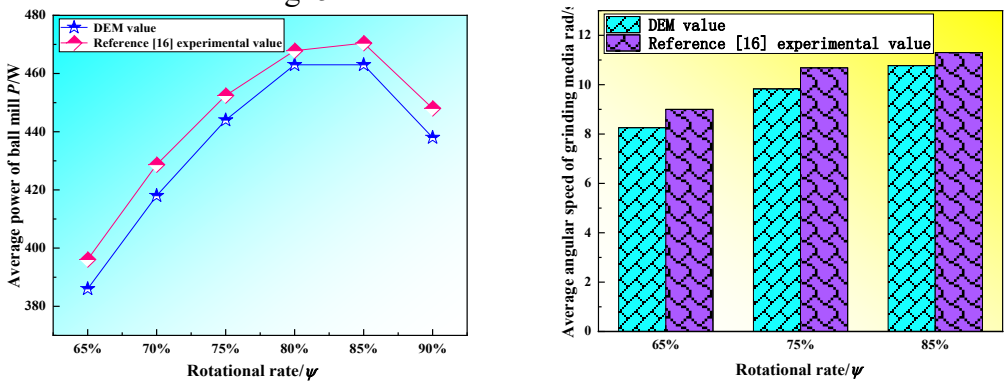

(a) Average power of ball mill (b) Average angular speed of grinding media

Fig. 5. Comparison between DEM simulation and literature [16]

As can be seen from Fig. 5, the simulation results tend to be consistent with the experimental results of literature [16]. With the increase of rotational rate, the average power shows a trend of increasing and then decreasing, and the average angular velocity of the grinding medium shows a trend of gradually increasing. It could be seen that the maximum relative errors of the average power and angular velocity of the grinding medium are 2.23% and 8.2%, respectively, which proves that the correctness of the discrete element model in this paper.

5. Results analysis

Fig. 6 gives particle flows at different operation state. As can be seen from Fig. 6, the running state of ball mill can be divided into three stages: falling stage, starting stage, and stabilization stage. Among them, the falling stage is mainly the generation stage of grinding media and ores, and the particles are mainly concentrated at the bottom of the cylinder due to the influence of gravity. The start-up stage is a acceleration process of the ball mill, in which the ores start to be lifted due to the operation of the ball mill, but at this time, due to the low

rotational speed, the ores and the grinding media mainly do lagging motion, and so the grinding efficiency is low. The stable stage is the operation state after the mill speed reaches the steady-state, in which due to the larger rotational speed, the ores and the grinding media mainly do throwing down motion, and the grinding efficiency is high.

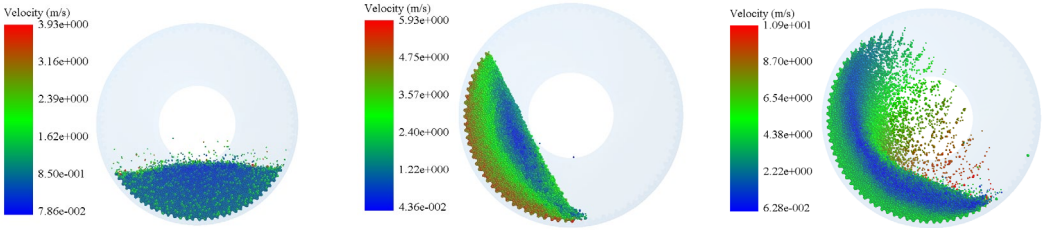

(a) blanking stage (b) start-up stage (c) stabilization stage

Fig. 6. Particle flows at different running state

5.1 Effect of rotational rate on operating efficiency

Suppose the rotational rates are 60%, 70%, 80% and 90%, the corresponding rotational speeds are equal to 9.50 r/min, 11.09 r/min, 12.67 r/min and 14.26 r/min, respectively. The liner height is 120 mm. Under these conditions, the number of inter-particle collisions and mill's useful power as well as impact force were calculated as shown in Fig. 7-9.

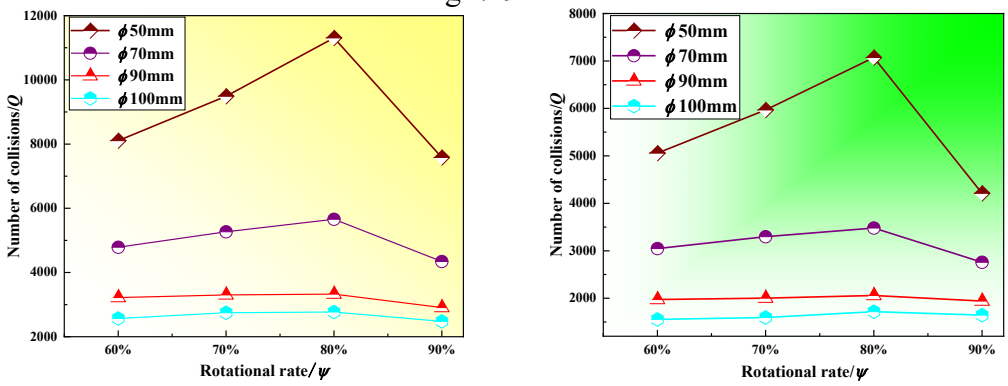

(a) Steel ball ϕ60 (b) steel ball ϕ80

Notes: ϕ50，ϕ60，ϕ90 and ϕ100 are different sizes of ore

Fig. 7. Collision number between steel ball and ores at different rotational rates

As can be seen from Fig. 7, the collisions number between the steel balls and ores increases and then decreases with the increase of rotational rate at the same corrugation height and the maximum collision number with the steel balls ϕ60 and ϕ80 are 11308 and 7072, respectively. Among the four rotational rates, the best one is 80%. In addition, the grinding media mainly does the lagging

motion when the rotational rate is equal to 60%. When the rotational rate is 100%, the media will do centrifugal motion. But with a 70% to 90% rotational rate, the mill mainly relies on the media's falling motion to improve the its efficiency. Therefore, the best rotation rate range is selected as 70%~90%.

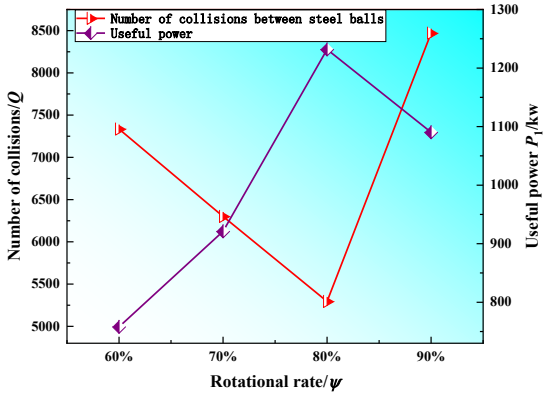

Fig. 8. Collision number between steel balls and useful power at different rotational rates

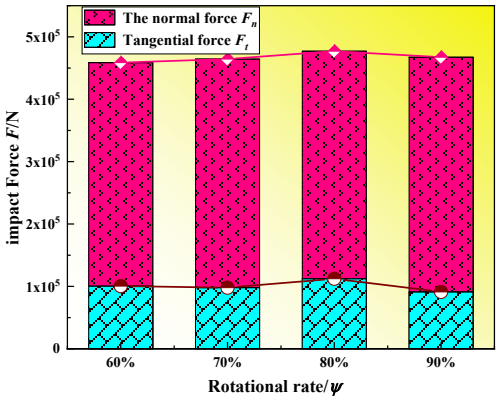

Fig. 9. Impact force at different rotational rates

From Fig. 8, it can be seen that under the same corrugation height, the collision number between steel balls first decreases and then increases with the increase of the rotational rate. However, the curve of useful power shows a trend of increasing first and then decreasing. The maximum useful power is gotten when the rotational rate is 80%. Since the collision between the steel balls is invalid, it is useless for grinding ore. Therefore, when the collision number between steel balls are the lowest, the useful power is conversely highest.

As can be seen from Fig. 9, the impact force shows a trend of first increasing and then decreasing with the increase of the rotational rate. The impact force of steel ball can be divided into tangential force and normal force, and only the normal force is used to crush the ores. Therefore, the larger the normal force is, the better the crushing effect is and the higher the grinding efficiency is. In this paper, the value of normal force is ranked as ψ=80%> ψ=90% > ψ=70%> ψ=60%. It can be concluded that the maximum normal force is 4.771×10^5N when the rotational rate is equal to 80%, indicating that the optimal rotational rate is between 70%~90%.

5.2 Effect of liner ripple height

When the rotational rate is 80%, the collision number and the useful power as well as impact force with different ripple heights of 80 mm, 100 mm, 120 mm and 140 mm are analyzed, respectively. The results are shown in Figure. 10 -12.

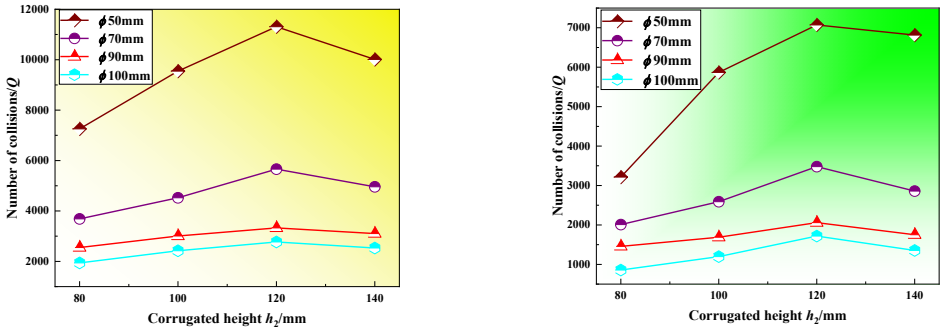

(a) steel ball ϕ60 (b) steel ball ϕ80

Notes: ϕ50，ϕ60，ϕ90 and ϕ100 are different sizes of ore

Fig. 10. Collision times of steel ball and ores at different ripple heights

Fig. 10 shows that the collision number between steel balls and ores first increases and then decreases with the increase of corrugation height. And when the corrugation height is 120mm, the maximum collision number of steel balls ϕ60 and ϕ80 are 11308 and 7072, respectively. And the best corrugation height range is 100~120 mm.

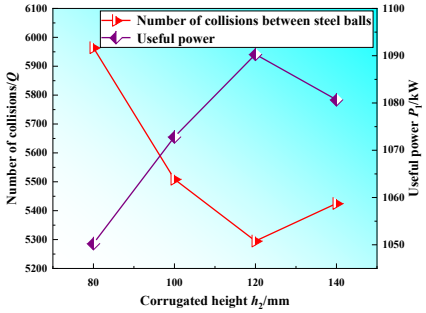

Fig. 11. Collision times and useful power between steel balls vary with ripple height

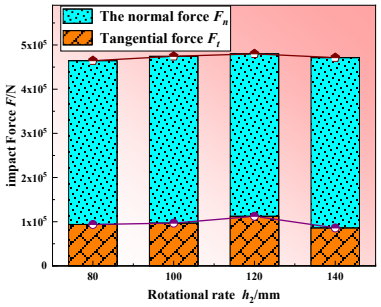

Fig. 12. Change curve of impact force with ripple height

As can be seen from Fig. 11, the collision number between steel balls decreases with ripple height of 80 and 120 mm, and starts to increase after ripple height 120 mm. But the useful power shows the trend of increasing first and then decreasing when the corrugation height changes. It can be concluded that when the corrugation height is 120mm, the useful power of the mill is the highest, which means the corrugated liner with the height of 120mm is the best, and at this time the mill efficiency is the highest and the grinding effect is the best. In addition, the best corrugation height is between 100~140mm.

As can be seen from Fig. 12, with the increase of corrugation height, the impact force shows a trend of increasing first and then decreasing. And the normal force is ranked as follows: h_2=120>h_2=140>h_2=100>h_2=80. It can be concluded that when the corrugation height is 120mm, the normal force of the mill is the

largest, and the maximum is 4.771×10^5N, indicating that the corrugated liner with a height of 120mm is the best, and the best corrugation height is between 100~140mm.

6. Conclusion

In this paper, the 3D model of the ball mill cylinder is created in Solid works, and then is imported into the EDEM. The correctness of the modeling method in this paper was verified by comparing the simulation with the experimental results in the literature [16]. Next, the number of particle collisions, useful power and impact force at different rotational rates and liner ripple height were analyzed. And the following conclusions can be drawn.

1) Under the same corrugation height, with the increase of rotational rate, the collision number of steel balls and ores, impact force, and useful power show a trend of increasing first and then decreasing, while the number of collisions between steel balls shows a trend of decreasing first and then increasing. The best rotational rate is between 70% and 90%.

2) Under the same rotation rate, with the increase of corrugation height, the collision number of steel balls and ores, impact force, and useful power show the trend of increasing first and then decreasing, while the number of collisions between steel balls shows the trend of decreasing first and then increasing. The best corrugation height is between 100~140mm.

The results of this paper could provide some reference for the optimization scheme of the ball mill.

Acknowledgements

The authors gratefully acknowledge the support from the Major scientific and technological projects in Shanxi Province(20201102003), Shanxi coal based low carbon joint fund （No.U1610118), National Natural Science Foundation of China (No. 51375325).

REFERENCES

[1] *S. Rosenkranz, S. Breitung-Faes, and A. Kwade.* "Experimental investigations and modelling of the ball motion in planetary ball mills". Powder Technology, **vol. 212**, no.1, 2011, pp.224-230.

[2] *D. W. Fuerstenau, A. Z. M. Abouzeid*. "The energy efficiency of ball milling in comminution". International Journal of Mineral Processing, **vol. 67**, no.1, 2002, pp.161-185.

[3] *M. Rezaeizadeh, M. Fooladi,and M. S. Powell, S. H. Mansouri, and N. S. Weerasekara*. " A new predictive model of lifter bar wear in mills". Minerals Engineering, **vol.23**, no.15, 2010, pp.1174-1181.

[4] *X.L. Bian*. Experimental study and DEM simulation on the effect of lifters on the behavior of tumbling ball mill, Master's thesis, Jilin University,2017.

[5] *P.W. Cleary*. "Predicting charge motion, power draw, segregation and wear in ball mills using discrete element methods". Minerals Engineering, **vol.11**, no.11, 1998, pp.1061-1080.

[6] *G.Z. Li, R. Roufail, B. Klein, L.S. Zhou, A. Kumar, Kumar, C.B. Sun, J. Kou and L. Yu*. "Investigations on the charge motion and breakage effect of the magnetic liner mill using DEM". Mining, Metallurgy & Exploration, **vol.36**, no.6, 2019, pp.1053-1065.

[7] *N.S. Weerasekara, M.S. Powell, P.W. Cleary, L.M. Tavares, M. Evertsson, R.D. Morrison, J. Quist and R.M. Carvalho*. "The contribution of DEM to the science of comminution". Powder Technology. **vol.248**, 2013, pp.3-24.

[8] *M. Liang, Y. Sun, Y, P.P. Ji, J.H. Shan and X.H. Jin*. "Numerical analysis on regular polygon angle-spiral liners design in a ball mill". Journal of Mechanical Engineering, **vol.51**, no.17, 2015, pp.203-212.

[9] *S.Q. Wang, X.Y. Cao and W.P. Duan*. "Design optimization of small ball mill liner in metal mines". Modern Mining, **vol.30**, no.7, 2014, pp.169-171.

[10] *S.S. Sun, W.M. Dong, Z.R. Wang, X.D. Zhang and H.Y. Zhou*. "The design of wave liner for sag mill based on EDEM and ANSYS coupling method". Mining and Metallurgy, **vol.27**, no.1, 2018, pp.61-65.

[11] *T.F. Li, S.Y. Lin, B. Zhang, J.M. Zhang, F. Jiao, W.Q. Tan and Y.S. Zhang*. "Study on collisions of steel balls in grinding mill at different rotation speeds". Journal of Central South University (Science and Technology), **vol.50**, no.2, 2019, pp.251-256.

[12] *P.W. Cleary*. "Charge behavior and power consumption in ball mills: sensitivity to mill operating conditions, liner geometry and charge composition". International Journal of Mineral Processing, **vol.63**, no.2, 2000, pp.79-114.

[13] *P.W. Cleary, D. Hoyer*. "Centrifugal mill charge motion and power draw: comparison of DEM predictions with experiment". International Journal of Mineral Processing, **vol.59**, no.2, 2000, pp. 131-148.

[14] *P.W. Cleary*. "Sinnott, M.D., Morrison, R.D., "DEM prediction of particle flows in grinding processes". International Journal for Numerical Methods in Fluids, **vol.58**, no.3, 2004, pp. 319-353.

[15] *S*.Y.Zhao. "Study on the Influence of Ball Mill Speed and Grinding Ball Size on Efficiency and Energy Consumption". Master's thesis, Taiyuan University of Science and Technology University,2017.

[16] *Z.X. Yin*. "Study on breakage and size distribution behavior of Iron ore particle in ball mills, PhD dissertation, China University of Mining and Technology,2020.